JOINT INSTITUTE FOR AERONAUTICS AND ACOUSTICS

STANFORD UNIVERSITY

AMES RESEARCH CENTER

JIAA TR - 17
and
NASA CR - 152244

FLAP-LAG-TORSION FLUTTER ANALYSIS OF A CONSTANT LIFT ROTOR

(NASA-CR-152244) FLAP-LAG-TORSION FLUTTER ANALYSIS OF A CONSTANT LIFE ROTOR (Stanford Univ.) 42 p HC A03/MF A01 CSCL 01C

N79-20099

Unclas

G3/05 16663

INDERJIT CHOPRA

JANUARY 1979

JIAA TR - 17

and

NASA CR - 152244

FLAP-LAG-TORSION FLUTTER ANALYSIS OF A CONSTANT LIFT ROTOR

INDERJIT CHOPRA

JANUARY 1979

The work here presented has been supported by the National Aeronautics and Space Administration under NASA Grant No. NSG - 2317 to the Joint Institute of Aeronautics and Acoustics.

ABSTRACT

The constant lift rotor (CLR) employs a control input of pitch moment to several airfoil sections which are free to pivot on a continuous spar, allowing them to change their pitch to obtain the desired lift. A flap-lag-torsion flutter analysis of a constant lift rotor blade in hover was developed. The blade model assumes rigid body flap and lead-lag motions at the root hinge and each strip undergoes an independent torsional motion. The results are presented in terms of root locus plots of complex eigenvalues as a function of thrust. The effects of several parameters (including strucural damping, center of gravity and elastic axis offset from aerodynamic center, compressibility, pitch-lag and pitch-flap coupling) on the blade dynamics are examined. With a suitable combination of lag damper and pitch-flap coupling, it is possible to design a constant lift rotor blade free from flutter instability.

ACKNOWLEDGEMENT

The author wishes to acknowledge helpful discussions and valuable suggestions with Wayne Johnson and Robert H. Stroub. The constant lift rotor is an invention of Robert H. Stroub (U.S. Patent 4137010 January 30, 1979).

The work reported here is sponsored by NASA Ames Research Center, under NASA Grant NSG-2317. The technical monitor is David H. Hickey, Large Scale Aerodynamics Branch, NASA Ames Research Center.

TABLE OF CONTENTS

ABSTRACT ii

ACKNOWLEDGEMENT iii

SYMBOLS v

INTRODUCTION 1

EQUATIONS OF MOTION 2

PITCH-LAG AND PITCH-FLAP COUPLING 9

RESULTS AND DISCUSSION 10

CONCLUSIONS 13

APPENDIX 14

FIGURES 20

SYMBOLS

a_r	Reference lift-curve slope (5·7/rad)
c	Chord
c_d	Blade section drag coefficient
c_ℓ	Blade section lift coefficient
c_m	Blade section moment coefficient
C_T	Rotor thrust coefficient, $T/\pi\rho\Omega^2R^4$
D	Blade section drag force
e	Hing offset from rotation axis in terms of blade length ℓ
$g_\beta, g_\zeta, g_\theta$	Structural damping coefficients
I_b	Moment of inertia of blade (flap)
ℓ	Length of blade from hinge
L	Blade section lift force
M_{ac}	Blade section aerodynamic moment about aerodynamic center
M	Mach number
$Q_\beta, Q_\zeta, Q_{\theta_i}$	Perturbation aerodynamic moments at hinge
Q_{β_o}, Q_{ζ_o}	Steady aerodynamic moments at hinge
r	Blade radial station (from hinge)
R	Rotor blade radius
R_β	Pitch-flap coupling parameter
R_ζ	Pitch-lag coupling parameter
R_{m_i}	Ratio of torsional inertia of i^{th} strip to blade flap inertia
s_i	Strip width (i^{th}) in terms of blade length ℓ
T	Rotor thrust force

u_P Blade section normal velocity

u_T Blade section inplane velocity

V Blade section resulant velocity

X_{A_e} Chordwise offset of pitch axis from aerodynamic center (positive forward)

X_{cg} Chordwise offset of cg from pitch axis in terms of blade length (positive aft pitch axis)

α Blade section angle of attack

β, ζ, θ_i Angular deflections

β_o, ζ_o Static deflections

β_p Precone

β_s, ζ_s Initial settings

γ Blade lock number, $\rho a_r c \ell^4 / I_b$

θ_{oi} Built-in twist

λ_i Rotor inflow ratio

$\nu_\beta, \nu_\zeta, \nu_{\theta_i}$ Nonrotating natural frequencies of blade

ξ_i Nondimensional coordinate, r_i/ℓ

ρ Air density

σ Solidity ratio

ϕ Induced angle, $\tan^{-1} u_p/u_T$

Ω Rotor rotational speed

INTRODUCTION

In conventional rotors, lift variation is achieved by pitch control input to blades. For a constant lift rotor (CLR), the lift variation is achieved through a control input of pitching moment to the blade and allowing the blade to change its pitch. This helps to alleviate the oscillatory loads on the rotor.

Constant lift rotor employs a finite number of segments pivotally mounted on a continuous spar and the pitch of each segment is determined by the balance of centrifugal, aerodynamic, control, and frictional forces. Each one of the airfoil strips is directed through a control rod to achieve a desired amount of lift. There is chordwise offset of elastic axis from aerodynamic center (forward direction) and the strips can float freely torsionally.

In the present paper, the flap-lag-torsion flutter of a constant lift rotor blade in hovering is investigated. The equations of motion for the shaft-fixed dynamics are derived for a blade with finite number of spanwise strips. These equations are linearized about a trim static solution in hover. The blade is assumed to have rigid body flap and lead-lag motions at the root hinge and, also, each one of the segments can undergo independent torsional motion. Quasi-static airfoil characteristics are used to obtain aerodynamic forces (stalling is not considered, however). The results are presented in form of root locus plots of complex eigenvalues as a function of c_T/σ. The effects of structural damping, cg and elastic axis offset from aerodynamic center, compressibility correction, pitch-flap and pitch-lag coupling are studied.

EQUATIONS OF MOTION

Fig. 1 presents the blade configuration considered for the analysis. The blade consists of N rigid strips, M connected to spar through torsional springs, and its flap and lead-lag stiffnesses are represented by springs at hinges offset by a distance $e\ell$ from the hub. The hinge sequence is flap inboard, lead-lag and then torsional motions outboard. The flap angle β is positive up, the lead-lag ζ is positive forward, and the pitch angles θ_i are positive nose up. The hub has a precone angle β_p. The blade rotates at a constant rotational speed Ω.

The linear equations of motion are derived by assuming the response consists of small perturbation motion $(\beta, \zeta, \theta_1, \ldots \theta_N)$ about a steady deflection (β_o, ζ_o). In general, terms up to second order are retained in flap and lag equations, terms up to third order are retained in torsion equations.

Flap eqn.:

$$\ddot{\beta} + 2(\beta_o+\beta_p)\dot{\zeta} + (1+\frac{3}{2}e+\nu_\beta^2)\beta + g_\beta\dot{\beta} - \sum_1^N R_{m_i}\zeta_o(\ddot{\theta}_i+\theta_i)$$

$$-\frac{3}{2}\sum_1^N \chi_{cg_i} s_i(\xi_i+\xi_{i+1})(\ddot{\theta}_i+\theta_i) = Q_\beta/I_b\Omega^2 \qquad (1)$$

Lag eqn.:

$$\ddot{\zeta} - 2(\beta_o+\beta_p)\dot{\beta} + (\frac{3}{2}e+\nu_\zeta^2)\zeta + g_\zeta\dot{\zeta} - \sum_1^N R_{m_i}(\beta_o+\beta_p)\theta_i$$

$$+\frac{3}{2}\sum_1^N \chi_{cg_i} s_i(\xi_i+\xi_{i+1})\{\theta_{oi}\ddot{\theta}_i+2(\beta_o+\beta_p)\dot{\theta}_i\} = Q_\zeta/I_b\Omega^2 \qquad (2)$$

Torsion eqn.: (i^{th} strip)

$$R_{m_i}\{\ddot{\theta}_i-\zeta_o\ddot{\beta}+(1+\nu_{\theta_i}^2)\theta_i - (\beta_o+\beta_p)\zeta-\zeta_o\beta+g_{\theta_i}\dot{\theta}\}$$

$$+3\chi_{cg_i}\{\chi_{cg_i}s_i\ddot{\theta}_i-\frac{1}{2}s_i(\xi_i+\xi_{i+1})(\ddot{\beta}+\beta)+\frac{1}{2}s_i(\xi_{i+1}+\xi_i)[\theta_{oi}\ddot{\zeta}-2(\beta_o+\beta_p)\dot{\zeta}]\}$$

$$= Q_\theta/I_b\Omega^2 \qquad (3)$$

where R_{m_i} is the ratio of torsional inertia of i^{th} strip to blade inertia I_b; χ_{cg_i} is the ratio of the chordwise offset of cg and pitch axis to rotor radius (positive toward the trailing edge); $g_\beta, g_\zeta, g_{\theta_i}$ are the structural damping coefficients; $\nu_\beta, \nu_\zeta, \nu_{\theta_i}$ are the nonrotating natural frequencies of the blade (divided by Ω). It is assumed in the above derivations that the inertia properties are uniform within each strip and ξ_i and s_i respectively represent strip beginning from hinge and strip width in terms of blade length ℓ. The Q_β, Q_ζ and Q_{θ_i} are the perturbation aerodynamic moments.

The trim equations are:

$$(1+\frac{3}{2}e+\nu_\beta^2)\beta_o + (1+\frac{3}{2}e)\beta_p - \nu_\beta^2\beta_s - (\beta_o+\beta_p)\zeta_o^2 - \frac{3}{2}\sum_1^N \chi_{cg_i} s_i(\xi_i+\xi_{i+1})\theta_{oi}$$

$$= Q_{\beta_o}/I_b\Omega^2$$

$$(\frac{3}{2}e+\nu_\zeta^2)\zeta_o - \nu_\zeta^2\zeta_s - \frac{3}{2}\sum_1^N \chi_{cg_i} s_i(\xi_i+\xi_{i+1})e - (\beta_o+\beta_p)^2\zeta_o$$

$$= Q_{\zeta_o}/I_b\Omega^2 \qquad (4)$$

where β_s and ζ_s are the initial settings of flap and lag hinge springs (relative to the preconed hub). Q_{β_o} and Q_{ζ_o} are the steady aerodynamic moments at the hinges.

The aerodynamic forces are obtained using quasi-steady airfoil theory. The section lift, drag and moment about aerodynamic center are:

$$
\begin{aligned}
L &= \tfrac{1}{2}\rho V^2 c c_\ell(\alpha,M) \\
D &= \tfrac{1}{2}\rho V^2 c c_d(\alpha,M) \qquad (5) \\
M_{ac} &= \tfrac{1}{2}\rho V^2 c^2 c_m
\end{aligned}
$$

The section lift and drag coefficients c_ℓ and c_d are functions of section angle of attack and Mach number.

$$
\begin{aligned}
c_\ell &= (c_0+c_1\alpha)CR \\
c_d &= \delta_0 + \delta_1\alpha + \delta_2\alpha^2 + \Delta c_d \qquad (6) \\
c_m &= c_{m_o}
\end{aligned}
$$

The compressibility correction CR and Δc_d are

$$
\begin{aligned}
CR &= \frac{1}{\sqrt{1-M^2}} && M < M_c \\
&= \frac{1}{\sqrt{1-M_c{}^2}}\ \frac{1-M}{1-M_c} && M > M_c \qquad (7) \\
\Delta c_d &= 1.65(|\alpha|-\alpha_{div}) \\
&= 0 && |\alpha| < \alpha_{div}
\end{aligned}
$$

where

$$
\begin{aligned}
\alpha_{div} &= .26(M_d-M) \\
&= 0 && M > M_d
\end{aligned}
$$

M_c and M_d are respectively lift divergence and drag divergence Mach numbers.

Fig. 2 shows the section aerodynamic environment. The flow velocity components along the shaft axes are u_T and u_p and θ_{oi} in the pitch for the i^{th} strip. The resultant flow velocity is then $V = \sqrt{u_T^2 + u_p^2}$. The resolved aerodynamic moments in shaft axes are

$$\begin{aligned} N &= L\cos\phi - D\sin\phi \\ C &= L\sin\phi + D\cos\phi \\ M &= M_{ac} \end{aligned} \tag{8}$$

where ϕ is the induced angle of attack, $\tan^{-1} u_p / u_T$

The perturbation section aerodynamic forces and pitch moment are

$$\begin{aligned} \Delta N = \tfrac{1}{2}\rho c [\delta u_p \{ &-\frac{u_T}{V}(u_T c_{\ell_\alpha} - u_P c_{d_\alpha}) + \frac{u_P u_T}{V}(c_\ell + Mc_{\ell_M}) - c_d V \\ &- \frac{u_P^2}{V}(c_d + Mc_{d_M})\} \\ + \delta u_T \{ &\frac{u_P}{V}(u_T c_{\ell_\alpha} - u_P c_{d_\alpha}) + \frac{u_T^2}{V}(c_\ell + Mc_{\ell_M}) + c_\ell V \\ &- \frac{u_P u_T}{V}(c_d + Mc_{d_M})\} + \delta\theta_o\{V(u_T c_{\ell_\alpha} - u_P c_{d_\alpha})\}] \end{aligned} \tag{9}$$

$$\begin{aligned} \Delta C = \tfrac{1}{2}\rho c [\delta u_p \{ &-\frac{u_T}{V}(u_P c_{\ell_\alpha} + u_T c_{d_\alpha}) + \frac{u_P^2}{V}(c_\ell + Mc_{\ell_M}) + c_\ell V \\ &+ \frac{u_P u_T}{V}(c_d + Mc_{d_M})\} \\ + \delta u_T \{ &\frac{u_P}{V}(u_P c_{\ell_\alpha} + u_T c_{d_\alpha}) + \frac{u_P u_T}{V}(c_\ell + Mc_{\ell_M}) + c_d V \\ &+ \frac{u_T^2}{V}(c_d + Mc_{d_M})\} \\ + \delta\theta_o\{ &V(u_P c_{\ell_\alpha} + u_T c_{d_\alpha})\}] \end{aligned} \tag{10}$$

$$\Delta M_a = \tfrac{1}{2}\rho c^2 [\delta U_p\{-U_T c_{m_\alpha} + 2U_P c_m\}$$

$$+ \delta U_T\{U_p c_{m_\alpha} + 2U_T c_m\}$$

$$+ \delta\theta_o\{V^2 c_{m_\alpha}\} \tag{11}$$

and the steady forces are

$$N_o = \tfrac{1}{2}\rho c\{c_\ell U_T V - c_d U_p V\}$$

$$C_o = \tfrac{1}{2}\rho c\{c_\ell U_p V + c_d U_T V\} \tag{12}$$

The perturbation aerodynamic moments required for equations of motion are

$$Q_\beta = \int_o^\ell \{(1-\tfrac{1}{2}\zeta_o^2) r dN - r\zeta_o \zeta N_o - r\theta_i C_o$$

$$+ \chi_{A_e}\zeta_o(dN \cos\theta_{oi} + dC \sin\theta_{oi}) + \chi_{A_e}\zeta(N_o \cos\theta_{oi} + C_o \sin\theta_{oi})\}dr$$

$$Q_\zeta = -\int_o^\ell \{r dC + \theta_i r N_o\} dr \tag{13}$$

$$Q_{\theta_i} = -\int_{\xi_1\ell}^{\xi_2\ell} \{\chi_{A_e} \cos\theta_{oi} dN + \chi_{A_e} \sin\theta_{oi} dC + dM + M_{Nc}\}dr$$

and the steady aerodynamic moments are

$$Q_{\beta_o} = \int_o^\ell \{(1-\tfrac{1}{2}\zeta_o^2) r N_o + \chi_{A_e}\zeta_o(N_o \cos\theta_{oi} + C_o \sin\theta_{oi})\}dr$$

$$Q_{\zeta_o} = \int_o^\ell r C_o dr \tag{14}$$

where r is the radial distance from hinge and χ_{A_e} is the chordwise offset of pitch axis from aerodynamic center (positive forward). M_{NC} is the noncirulatory aerodynamic pitch moment due to unsteady thin airfoil theory.

$$M_{NC} = \frac{1}{4}\Pi\rho\bar{\Omega}^2c^3\{r(\frac{1}{4}+\frac{\chi_{A_e}}{c})\ddot{\beta} - r(\frac{1}{2}+\frac{\chi_{A_e}}{c})\dot{\theta} - c(\frac{3}{32}+\frac{1}{2}\frac{\chi_{A_e}}{c}+\frac{\chi_{A_e}^2}{c^2})\ddot{\theta}\} \tag{14}$$

The flow velocity components for hover are

$$\text{Steady:} \quad u_T = \Omega\ell\{(\xi+e) - \tfrac{1}{2}(\beta_o+\beta_p)^2\}$$
$$u_p = \Omega\ell\{\lambda_i + \xi(\beta_o+\beta_p)\zeta_o\} \tag{15}$$

$$\text{Perturbations:} \quad \delta u_T = \Omega\ell\{\xi\dot{\zeta} - \xi(\beta_o+\beta_p)\beta\}$$
$$\delta u_p = \Omega\ell\{\xi\dot{\beta} + \xi(\beta_o+\beta_p)\zeta + \xi\zeta_o\beta\} \tag{16}$$

and perturbation pitch for small angle assumption

$$\delta\theta_o = \theta_i + \frac{(\frac{1}{4}c+\chi_{A_e})}{(\xi+e)\ell}\dot{\theta}_i \tag{17}$$

where $\xi = r/\ell$ and λ_i is the wake induced inflow ratio (divided by $\Omega\ell$) and is assumed to be uniform within each strip for hovering condition. The λ_i is obtained by equating the thrust for i^{th} strip obtained from momentum theory and blade element theory for a specified load distribution:

$$\lambda_i = \sqrt{\frac{c_T}{2} \frac{f_i}{(\xi_{i+1}{}^2 - \xi_i{}^2)}} \tag{18}$$

where c_T is the thrust coefficient and f_i is the fractional thrust produced by i^{th} strip $(\Delta T_i = f_i T)$. The pitch settings are obtained as

$$\theta_{oi} = 6 \frac{c_T}{\sigma} f_i \left(\frac{1}{\xi_{i+1}{}^3 - \xi_i{}^3} \right) + \frac{3}{2} \lambda_i \frac{\xi_{i+1}{}^2 - \xi_i{}^2}{\xi_{i+1}{}^3 - \xi_i{}^3} \tag{19}$$

The resulting equations of motion for N-strips blade are

$$\begin{bmatrix} M_{11} & M_{12} & - & - & M_{1\,N+2} \\ M_{21} & M_{22} & - & - & M_{2\,N+2} \\ M_{31} & M_{32} & - & - & - \\ - & - & - & - & - \\ M_{N+2\,1} & M_{N+2\,2} & - & - & M_{N+2\,N+2} \end{bmatrix} \begin{bmatrix} \ddot{\beta} \\ \ddot{\zeta} \\ \ddot{\theta}_1 \\ - \\ \ddot{\theta}_N \end{bmatrix} \begin{bmatrix} C_{11} & C_{12} & - & - & C_{1\,N+2} \\ C_{21} & C_{22} & - & - & C_{2\,N+2} \\ C_{31} & C_{32} & - & - & C_{3\,N+2} \\ - & - & - & - & - \\ C_{N+2\,1} & - & - & - & C_{N+2\,N+2} \end{bmatrix} \begin{bmatrix} \dot{\beta} \\ \dot{\zeta} \\ \dot{\theta}_1 \\ - \\ \dot{\theta}_N \end{bmatrix}$$

$$\begin{bmatrix} K_{11} & K_{12} & - & - & K_{1\,N+2} \\ K_{21} & K_{22} & - & - & K_{2\,N+2} \\ K_{31} & K_{32} & - & - & K_{3\,N+2} \\ - & - & - & - & - \\ K_{N+2\,1} & K_{N+2\,2} & - & & K_{N+2\,N+2} \end{bmatrix} \begin{bmatrix} \beta \\ \zeta \\ \theta_1 \\ - \\ \theta_N \end{bmatrix} = 0 \tag{20}$$

The coefficients of these matrices are defined in appendix.

PITCH-LAG AND PITCH-FLAP COUPLING

For constant lift rotors, control input to individual blade strip is the pitch moment; thus, it is assumed here that the pitch-lag and pitch-flap coupling moments for each one of the strips are proportional to their torsional stiffness.

For i^{th} strip

$$m_{\theta_i} = - R_\beta K_{i+2\ i+2}\ \beta + R_\zeta K_{i+2\ i+2}\ \zeta$$

The pitch-flap coupling R_β is positive flap up, resulting in pitch down control moment and the pitch-lag R_ζ is positive lag back, resulting in pitch down control moment. The inclusion of these coupling moments modifies the stiffness matrix of resulting equations.

For i^{th} strip

Pitch-flap coupling

$$K_{i+2\ 1} = (K_{i+2\ 1})_o + R_\beta K_{i+2\ i+2}$$

Pitch-lag coupling

$$K_{i+2\ 2} = (K_{i+2\ 2})_o - R_\zeta K_{i+2\ i+2}$$

where $(\ )_o$ represents the blade without coupling.

RESULTS AND DISCUSSION

The flutter stability is examined for a constant lift rotor blade with lock number $\gamma = 8.65$; solidity ratio $\sigma = .088$; precone $\beta_p = 3.5°$; hinge offset $e = .04$; chord to radius ratio $c/R = .04$ and no droop or sweep. The following airfoil characteristics are used

$$c_\ell = 5.7\,\alpha$$

$$c_d = .008 + .023\,\alpha + .076\,\alpha^2$$

$$c_m = -.02$$

The constant lift rotor blade consists of five strips with the following properties

strip	1	2	3	4	5
strip width in radius, s_i	.6	.1	.1	.1	.1
Torsion inertia/Flap inertia R_{mi}	.00018	.00003	.00003	.00003	.00003
Thrust ratio, f_i	.35	.15	.17	.14	.14

For compressibility corrections, the lift divergence and drag divergence Mach numbers are assumed to be 0.7. Results are also presented for a conventional rotor blade (single strip) for comparision. Figure 3 shows the trim solution, the collective pitch as a function of thrust for constant lift rotor as well as conventional rotor. For dynamic results, the nondimensional eigenvalues (real and imaginary) are plotted in the complex plane for increasing thrust c_T/σ.

Figures 4-6 present the dynamic stability of a single strip blade. The first case considered is a conventional blade with torsion frequency of $\omega_\theta = 5$/rev and with no elastic axis/aerodynamic center offset $(x_{A_e} = 0)$ (Fig. 4). The blade is stable except near zero thrust level where lead-lag mode gets into a very weak instability. However, with zero torsion frequency $(\omega_\theta = 0)$ and zero elastic axis offset $(x_{A_e} = 0)$, the blade becomes very unstable (Fig. 5). The lead-lag instability expands up to higher thrust levels; and at still higher thrusts, torsion divergence takes place. With inclusion of elastic axis effect of $x_{A_e} = .12c$, the blade becomes torsionally stiff (due to aerodynamic forces) (Fig. 6). The lead-lag mode is still unstable and it becomes more and more violent with increasing level of thrust. The flap mode also gets into a weak instability at lower thrusts.

Figure 7 shows the results for a constant lift rotor blade with five strips, freely floating torsionally $(\omega_{\theta i} = 0)$, and with elastic axis offset $(x_{A_{e_i}} = .12c)$. All the seven eigenvalues are plotted here. The nature of two lowest damped modes which happen to be flap and lag modes is very similar to single strip case (see Fig. 4). The torsion modes of different segments are quite stable and therefore in subsequent figures only flap and lag modes are plotted.

In Figures 8(a)-(b), the effect of elastic axis offset from the aerodynamic center (x_{A_e}) on the blade dynamics of constant lift rotor is presented. For $x_{A_{e_i}} = .15c$, the flap and lead-lag modes are hardly different from those for the blade with $x_{A_{e_i}} = .12c$. The offset x_{A_e} primarily affects the different torsion modes, in fact, with increasing x_{A_e}, the torsional modes become stiffer, as expected.

Figures 9(a)-(b) show the influence of the cg offest from elastic axis, x_{cg} (positive toward trailing edge) on the blade dynamics. For $x_{cg_i} = .12c$ (cg coincidental with aerodynamic center), the flap and lag modes are changed very much and also torsional frequencies are reduced from that of the blade with $x_{cg_i} = 0$. (Fig. 9(a)). Also, for some lower thrusts, the lag mode gets into static divergence. For $x_{cg_i} = .06c$ (c.g. lying midway between the elastic axis and the aerodynamic center), the nature of flap and lag modes is quite similar to that of blade with $x_{cg_i} = 0$. (Fig. 9(b)).

In Figures 10-11, the influence of structural damping on the dynamics of constant lift rotor blade is shown. The flap mode instability, which was mild, can be easily stabilized with a low level of flap damper (Fig. 10). On the other hand, the lag mode instability becomes increasingly violent with higher thrusts, needs a fairly big lag damper to stabilize it (Figs. 11(a) and 11(b)).

Figures 12-18 show the effects of pitch-flap and pitch-lag coupling on the blade stability. The inclusion of positive pitch-flap coupling (pitch down moment with flap up) increases the cross coupling stiffness $(k_{i+2\ 1})$ for i^{th} strip. This destabilizes the flap mode somewhat (Fig. 12(a)). The opposite effect is seen with negative pitch-flap coupling which stabilizes the flap mode. (Fig. 12(b)). The addition of positive pitch-lag coupling (pitch down moment with lag back) stiffens the lag mode slightly, however, with little effect on its stability. (Fig. 13(a)). Again, with the negative pitch-lag coupling, the lag mode gets softened but the instability region is nearly the same (Fig. 13(b)).

Figure 14 shows the effect of compressibility for a blade with tip Mach number of $.6(\chi_{A_e} = .12C)$. The general behavior is similar to the blade reglecting the compressibility effects, particularly for low thrusts.

Figure 15 presents the blade dynamics with a suitable combination of lag damper $(g_\zeta = .5)$ and pitch-flap coupling $(R_\beta = -.3)$ for a constant lift rotor $(\chi_{A_{e_i}} = .12C,\ \chi_{cg_i} = 0)$. The blade is quite stable in the covered range of thrust. The same combination of lag damper and pitch-flap coupling is also used for another blade configuration $(\chi_{A_{e_i}} = .12C,\ \chi_{cg_i} = .06C)$. In Figure 16 the blade is shown to be stable except at very high thrusts $(\frac{C_T}{\sigma} > .2)$ the lag mode gets into static divergence.

CONCLUSIONS

The flap-lag-torsion flutter of a constant lift rotor in hover has been investigated. The CLR blade consists of a finite number of strips pivotally mounted on the spar and their torsional stiffness is attained through the elastic axis offset from the aerodynamic center. The perturbation equations of motion were derived, retaining the higher order steady terms. The dynamic results for multi-strip constant lift rotor are quire similar to those of a single strip blade under the same environment.

The effects of several parameters on the blade dynamics were examined, including structural damping, cg and elastic axis offset from aerodynamic center, compressibility correction, pitch-lag and pitch-flap coupling. With a suitable combination of lag damper and pitch-flap coupling, it is possible to design a constant lift rotor blade free from aeroelastic instability.

APPENDIX

1. Inertia Matrix "M"

$$\boxed{k = i+2}$$

$$M_{11} = 1.0$$

$$M_{12} = 0$$

$$M_{1k} = -\frac{3}{2} x_{cg_i} s_i (\xi_i + \xi_{i+1}) - R_{m_i} I_0$$

$$M_{21} = 0$$

$$M_{22} = 0$$

$$M_{2k} = \frac{3}{2} x_{cg_i} s_i (\xi_i + \xi_{i+1}) \theta_{0i}$$

$$M_{k1} = -\frac{3}{2} x_{cg_i} s_i (\xi_i + \xi_{i+1}) - R_{m_i} I_0 - \frac{\gamma}{8} \frac{c}{R} \left(\frac{1}{4} \frac{c}{R} + \frac{x_{Aei}}{R} \right) I_2$$

$$M_{k2} = \frac{3}{2} x_{cg_i} s_i (\xi_i + \xi_{i+1}) \theta_{0i}$$

$$M_{kk} = R_{m_i} + 3 x_{cg_i}^2 s_i + \frac{\gamma}{8} \frac{c}{R} \left[\frac{3}{32} \left(\frac{c}{R} \right)^2 + \frac{1}{2} \frac{x_{Aei}}{R} \frac{c}{R} + \left(\frac{x_{Aei}}{R} \right)^2 \right] I_1$$

2. Damping Matrix "C"

(a) Structure

$$C_{11} = g_\beta$$

$$C_{12} = 2(\beta_0 + \beta_p)$$

$$C_{1k} = 0$$

$$C_{21} = -2(\beta_0 + \beta_p)$$

$$C_{22} = g_\zeta$$

$$C_{2k} = 3\, x_{cg_i} s_i \left(\xi_i + \xi_{i+1} \right)\left(\beta_0 + \beta_p \right)$$

$$C_{k1} = 0$$

$$C_{k2} = -3\, x_{cg_i} s_i \left(\xi_i + \xi_{i+1} \right)\left(\beta_0 + \beta_p \right)$$

$$C_{kk} = R_{m_i}\, g_{\theta_i}$$

(b) Aerodynamics

$$C_{11} = -\frac{\gamma}{2} \Big[I_4 \left\{ \beta_T \zeta_0 R_1 + \left(1 - \tfrac{1}{2}\beta_T^2 - \tfrac{1}{2}\zeta_0^2\right) R_2 \right\} + I_3 \left\{ \lambda_i R_1 + e R_2 + \bar{x}_{Ae_i} \zeta_0 R_2 \cos\theta_{0i} \right\} \Big]$$

$$C_{12} = -\frac{\gamma}{2} \sum_1^N \Big[I_4 \left\{ \beta_T \zeta_0 R_3 + \left(1 - \beta_T^2 - \tfrac{1}{2}\zeta_0^2\right) R_4 \right\} + I_3 \left\{ \lambda_i R_3 + e R_4 + \bar{x}_{Ae_i} \zeta_0 R_4 \cos\theta_{0i} \right\} \Big]$$

$$C_{1k} = -\frac{\gamma}{2} \bar{\eta} \Big[I_3 \left\{ R_5 \left(1 - \tfrac{1}{2}\beta_T^2\right) + \beta_T \zeta_0 R_6 \right\} + I_2 \left\{ e R_5 + \lambda_i R_6 + x_{Ae_i} \zeta_0 R_5 \cos\theta_{0i} \right\} \Big]$$

$$C_{21} = \frac{\gamma}{2} \sum_1^N \Big[I_4 \left\{ \beta_T \zeta_0 S_1 + \left(1 - \tfrac{1}{2}\beta_T^2\right) S_2 \right\} + I_3 \left\{ \lambda_i S_1 + e S_2 \right\} \Big]$$

$$C_{22} = \frac{\gamma}{2} \sum_1^N \Big[I_4 \left\{ \beta_T \zeta_0 S_3 + \left(1 - \tfrac{1}{2}\beta_T^2\right) S_4 \right\} + I_3 \left\{ \lambda_i S_3 + e S_4 \right\} \Big]$$

$$C_{2k} = \frac{\gamma}{2} \bar{\eta} \Big[I_3 \left\{ \beta_T \zeta_0 S_6 + \left(1 - \tfrac{1}{2}\beta_T^2\right) S_5 \right\} + I_2 \left(\lambda_i S_6 + e S_5 \right) \Big]$$

$$C_{k1} = -\frac{\gamma}{2} \Big[I_2 \left(\lambda_i T_1 + e T_2 \right) + I_3 \left\{ \beta_T \zeta_0 T_1 + \left(1 - \tfrac{1}{2}\beta_T^2\right) T_2 \right\} \Big]$$

$$C_{k2} = -\frac{\gamma}{2} \Big[I_2 \left(\lambda_i T_3 + e T_4 \right) + I_3 \left\{ \beta_T \zeta_0 T_3 + \left(1 - \tfrac{1}{2}\beta_T^2\right) T_4 \right\} \Big]$$

$$C_{kk} = -\frac{\gamma}{2} \bar{\eta} \Big[I_2 \left\{ T_5 \left(1 - \tfrac{1}{2}\beta_T^2\right) + \beta_T \zeta_0 T_6 \right\} + I_1 \left(e T_5 + \lambda_i T_6 \right) \Big] + \frac{\gamma}{8} \frac{c}{R} \left(\frac{1}{2}\frac{c}{R} + \frac{x_{Ae_i}}{R} \right) I_2$$

3. **Stiffness Matrix "K"**

(a) Structure

$$K_{11} = 1 + \frac{3}{2} e + \nu_\beta^2$$

$$K_{12} = 0$$

$$K_{1k} = -\frac{3}{2} x_{cg_i} s_i (\xi_i + \xi_{i+1}) - R_{m_i} \zeta_o$$

$$K_{21} = 0$$

$$K_{22} = \frac{3}{2} e + \nu_\zeta^2$$

$$K_{2k} = -R_{m_i} (\beta_o + \beta_p)$$

$$K_{k1} = -R_{m_i} \zeta_o - \frac{3}{2} x_{cg_i} s_i (\xi_i + \xi_{i+1})$$

$$K_{k2} = -R_{m_i} (\beta_o + \beta_p)$$

$$K_{kk} = R_{m_i} (1 + \nu_{\theta_i}^2)$$

(b) Aerodynamics

$$K_{11} = -\frac{\gamma}{2} \sum_1^N \left[I_3 \{ \zeta_o (\lambda_i R_1 + e R_2) - \beta_T (\lambda_i R_3 + e R_4) \} + I_4 (\zeta_o R_2 - \beta_T R_4) \right]$$

$$K_{12} = -\frac{\gamma}{2} \sum_1^N \left[I_3 \{ \beta_T (\lambda_i R_1 + e R_2) \} + I_4 \beta_T R_2 - \zeta_o A_N \right.$$
$$\left. + \bar{x}_{Ae_i} (B_N \cos \theta_{oi} + B_c \sin \theta_{oi}) \right]$$

$$K_{1k} = -\frac{\gamma}{2} \left[I_4 \{ R_5 (1 - \beta_T^2) + \beta_T \zeta_o R_6 \} + I_3 \{ 2e (1 - \tfrac{1}{2} \beta_T^2) R_5 \right.$$
$$+ (\lambda_i + e \beta_T \zeta_o - \frac{1}{2} \lambda_i \beta_T^2) R_6 + 2 \beta_T \zeta_o \lambda_i R_7 + \bar{x}_{Ae_i} \zeta_o R_5 \cos \theta_{oi} \}$$
$$\left. + I_2 \{ e^2 R_5 + e \lambda_i R_6 + \lambda_i^2 R_7 \} - A_c \right]$$

$$K_{21} = \frac{\gamma}{2} \sum_{1}^{N} \left[I_3 \left\{ \zeta_0 (\lambda_i S_1 + e S_2) - \beta_T (\lambda_i S_3 + e S_4) \right\} + I_4 (\zeta_0 S_2 - \beta_T S_4) \right]$$

$$K_{22} = \frac{\gamma}{2} \sum_{1}^{N} \left[I_3 \left\{ \beta_T (\lambda_i S_1 + e S_2) \right\} + I_4 (\beta_T S_2) \right]$$

$$K_{2k} = \frac{\gamma}{2} \left[I_4 \left\{ (1 - \tfrac{1}{2} \beta_T^2) S_5 + \beta_T \zeta_0 S_6 \right\} + I_3 \left\{ 2e (1 - \tfrac{1}{2} \beta_T^2) S_5 \right. \right.$$
$$\left. \left. + (\lambda_i + e \beta_T \zeta_0 - \tfrac{1}{2} \lambda_i \beta_T^2) S_6 \right\} + I_2 \left\{ e^2 S_5 + \lambda_i e S_6 \right\} + A_N \right]$$

$$K_{k1} = -\frac{\gamma}{2} \left[I_2 (\lambda_i \zeta_0 T_1 + e \zeta_0 T_2 - \lambda_i \beta_T T_3 - e \beta_T T_4) + I_3 (\zeta_0 T_2 - \beta_T T_4) \right]$$

$$K_{k2} = -\frac{\gamma}{2} \left[I_2 (\lambda_i \beta_T T_1 + e \beta_1 T_2) + I_3 \beta_T T_2 \right]$$

$$K_{kk} = -\frac{\gamma}{2} \left[I_3 \left\{ (1 - \beta_T^2) T_5 + \beta_T \zeta_0 T_6 \right\} + I_2 \left\{ 2e (1 - \tfrac{1}{2} \beta_T^2) T_5 + 2 \beta_T \zeta_0 \lambda_i T_7 \right. \right.$$
$$\left. \left. + (\lambda_i + e \beta_T \zeta_0 - \tfrac{1}{2} \lambda_i \beta_T^2) T_6 \right\} + I_1 \left\{ e^2 T_5 + \lambda_i^2 T_7 + \lambda_i e T_6 \right\} \right]$$

where

$$\beta_T = \beta_0 + \beta_p$$

$$\bar{x}_{Ae_i} = x_{Ae_i} / \ell$$

$$\bar{\eta} = (x_{Ae_i} + \tfrac{1}{2} c) / \ell$$

$$R_1 = 2 (d_1 + 2 d_2 \theta_{0i} + dC_1^*) + (c_0 + C_1 \theta_{0i})(CR + M \, CR_M)$$

$$R_2 = -C_1 \, CR - (d_0 + d_1 \theta_{0i} + d_2 \theta_{0i}^2 + dC_s)$$

$$R_3 = -C_1 (CR + M \, CR_M) - (d_0 + d_1 \theta_{0i} + d_2 \theta_{0i}^2 + dC_s + M \, dC_2)$$

$$R_4 = (c_0 + C_1 \theta_{0i})(2 \, CR + M \, CR_M)$$

$$R_5 = C_1 \, CR$$

$$R_6 = -(d_1 + 2 d_2 \theta_{0i} + dC_1^*)$$

$$R_7 = 2 d_2$$

$$S_1 = -2C_1\, CR + 2d_2 + (d_0 + d_1\theta_{0i} + d_2\theta_{0i}^2 + dC_s) + M\, dC_2$$

$$S_2 = (C_0 + C_1\theta_{0i})\, CR - (d_1 + 2d_2\theta_{0i} + dC_1^*)$$

$$S_3 = -(d_1 + 2d_2\theta_{0i} + dC_1^*) + (C_0 + C_1\theta_{0i})(CR + M\; CR_M)$$

$$S_4 = 2(d_0 + d_1\theta_{0i} + d_2\theta_{0i}^2 + dC_s) + M\, dC_2$$

$$S_5 = (d_1 + 2d_2\theta_{0i} + dC_1^*)$$

$$S_6 = C_1\, CR - 2d_2$$

$$T_1 = 2\frac{c}{\ell} C_{m_0} - \frac{x_{Ae_i}}{\ell} R_1 \cos\theta_{0i} - \frac{x_{Ae_i}}{\ell} S_1 \sin\theta_{0i}$$

$$T_2 = -\frac{x_{Ae_i}}{\ell}(R_2\cos\theta_{0i} + S_2\sin\theta_{0i})$$

$$T_3 = -\frac{x_{Ae_i}}{\ell}(R_3\cos\theta_{0i} + S_3\sin\theta_{0i})$$

$$T_4 = 2\frac{c}{\ell} C_{m_0} - \frac{x_{Ae_i}}{\ell}(R_4\cos\theta_{0i} + S_4\sin\theta_{0i})$$

$$T_5 = -\frac{x_{Ae_i}}{\ell}(R_5\cos\theta_{0i} + S_5\sin\theta_{0i})$$

$$T_6 = -\frac{x_{Ae_i}}{\ell}(R_6\cos\theta_{0i} + S_6\sin\theta_{0i})$$

$$T_7 = -\frac{x_{Ae_i}}{\ell}(R_7\cos\theta_{0i} + S_7\sin\theta_{0i})$$

$$A_N = TR_1(I_4 + 2e\, I_3) + TR_2\lambda_i^2 I_2 + TR_3(\beta_T\zeta_0 I_4 + \lambda_i I_3 + e\lambda_i I_2)$$

$$B_N = TR_1(I_3 + 2e\, I_2) + TR_2\lambda_i^2 I_1 + TR_3(\beta_T\zeta_0 I_3 + \lambda_i I_2 + e\lambda_i I_1)$$

$$A_C = TR_4(I_4 + 2e\, I_3) + TR_5\lambda_i^2 I_2 + TR_6(\beta_T\zeta_0 I_4 + \lambda_i I_3 + e\lambda_i I_2)$$

$$B_c = TR_4 \left(I_3 + 2e\, I_2 \right) + TR_5\, \lambda_i^2\, I_1 + TR_6 \left(\beta_T \zeta_0\, I_3 + \lambda_i I_2 + e \lambda_i I_1 \right)$$

$$TR_1 = \left(C_0 + C_1\, \theta_{0i} \right) CR$$

$$TR_2 = -C_1\, CR - \left(d_0 + d_1\, \theta_{0i} + d_2\, \theta_{0i}^2 + dC_s \right)$$

$$TR_3 = d_1 + 2\, d_2\, \theta_{0i} + dC_1^*$$

$$TR_4 = d_0 + d_1\, \theta_{0i} + d_2\, \theta_{0i}^2 + dC_s$$

$$TR_5 = \left(C_0 + C_1\, \theta_{0i} \right) CR - \left(d_1 + 2\, d_2\, \theta_{0i} + dC_1^* \right)$$

$$TR_6 = -C_1\, CR$$

$$I_1 = \xi_{i+1} - \xi_i$$

$$I_2 = \frac{1}{2} \left(\xi_{i+1}^2 - \xi_i^2 \right)$$

$$I_3 = \frac{1}{3} \left(\xi_{i+1}^3 - \xi_i^3 \right)$$

$$I_4 = \frac{1}{4} \left(\xi_{i+1}^4 - \xi_i^4 \right)$$

$$dC_1^* = 1.65\, \alpha / |\alpha|$$

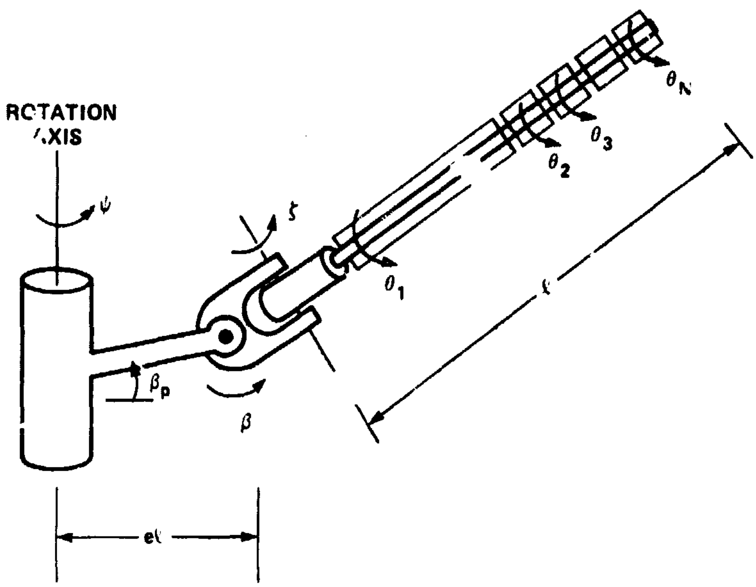

Figure 1.- Schematic of the N-strips blade model considered; the hinge sequence is flap, lag, torsions; flap motion β positive up, lead-lag motion ζ positive forward, torsion θ_i positive nose up.

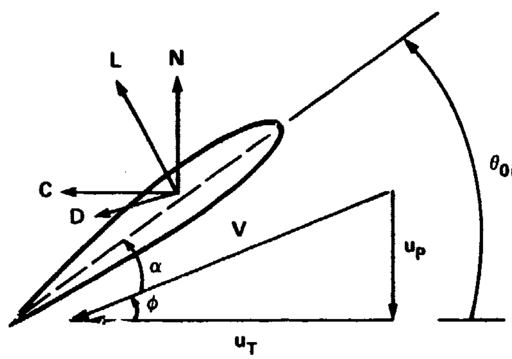

Figure 2.- Blade section aerodynamics.

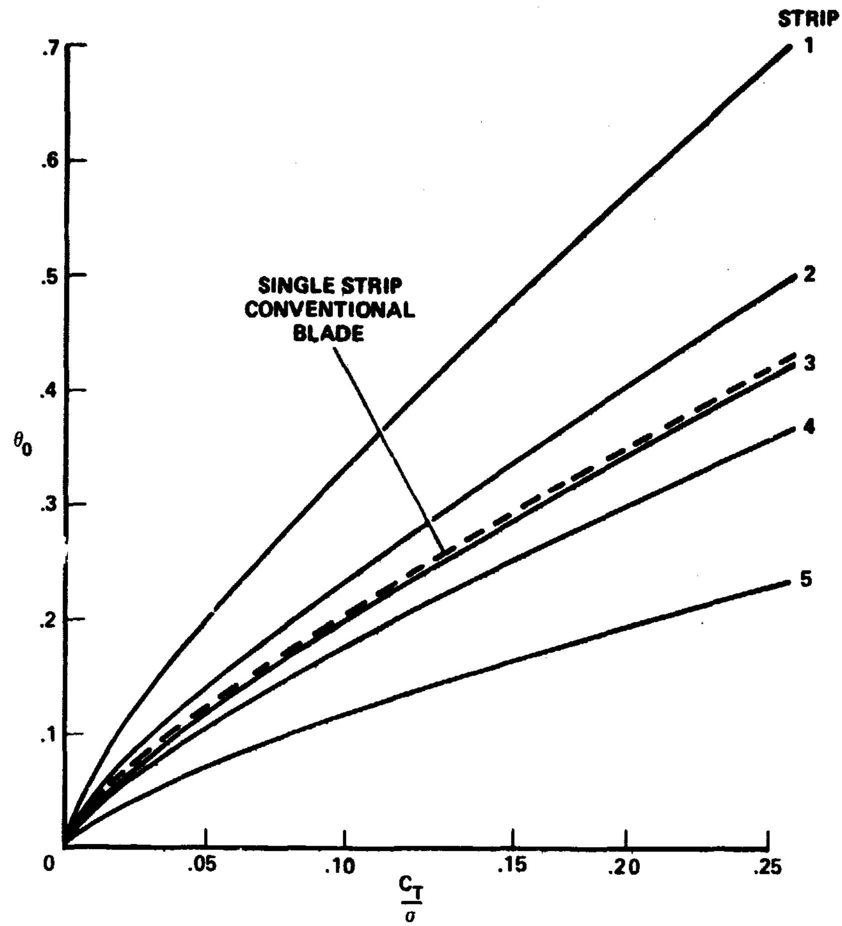

Figure 3.- Pitch settings for individual strips as a function of thrust.

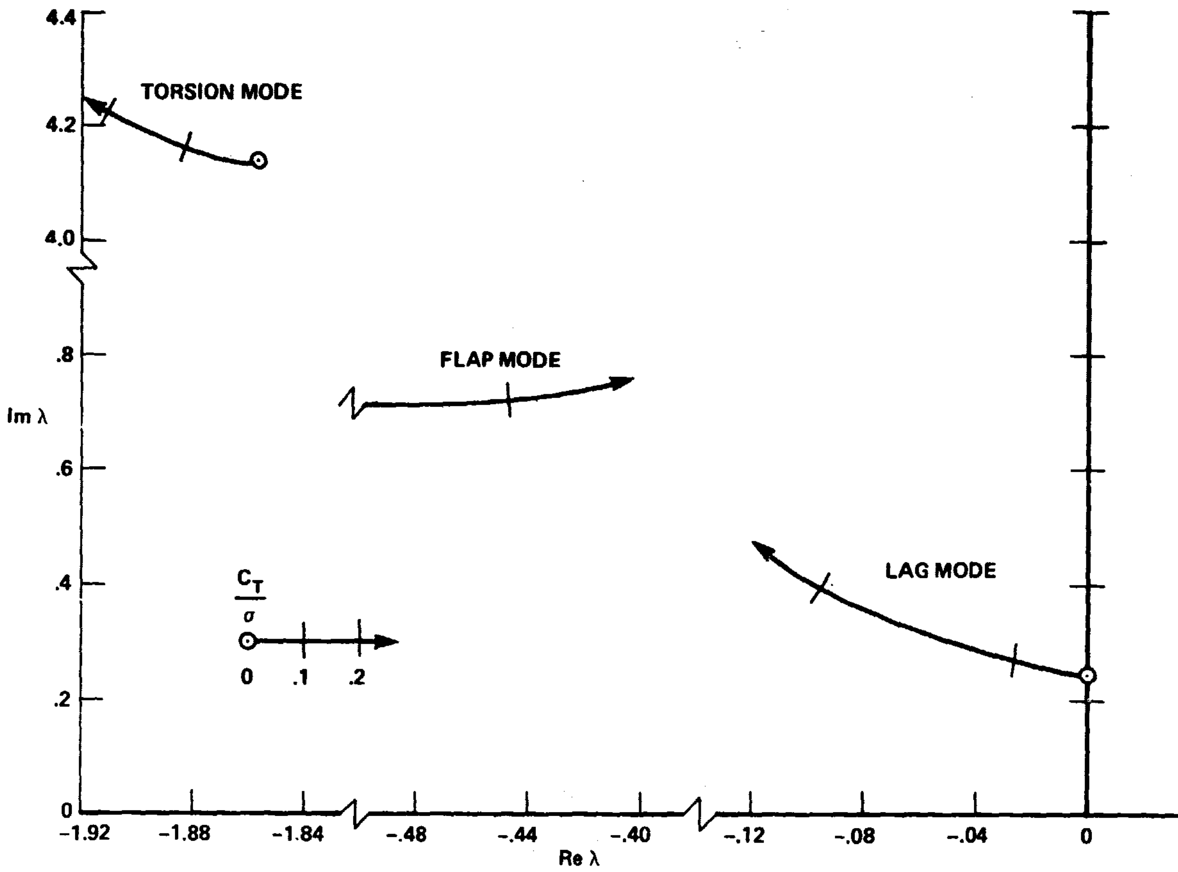

Figure 4.- Root loci for a single strip (conventional) blade for ω_θ = 5 and X_{A_e} = 0

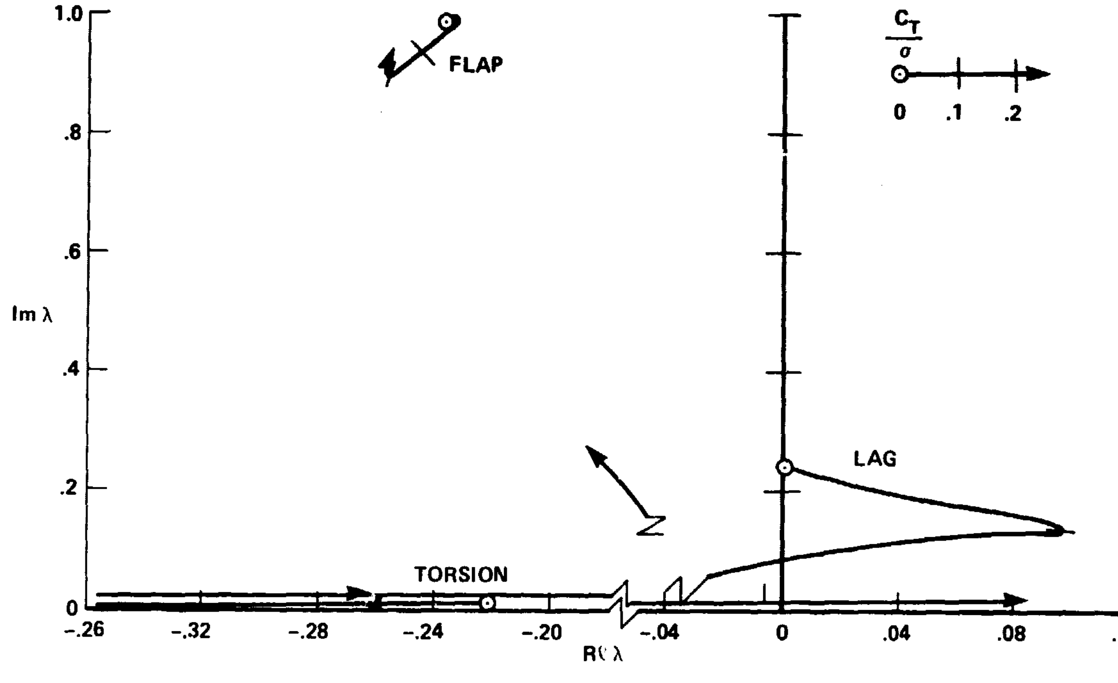

Figure 5.- Root loci for a single strip blade for $\omega_\theta = 0$ and $X_{A_e} = C$

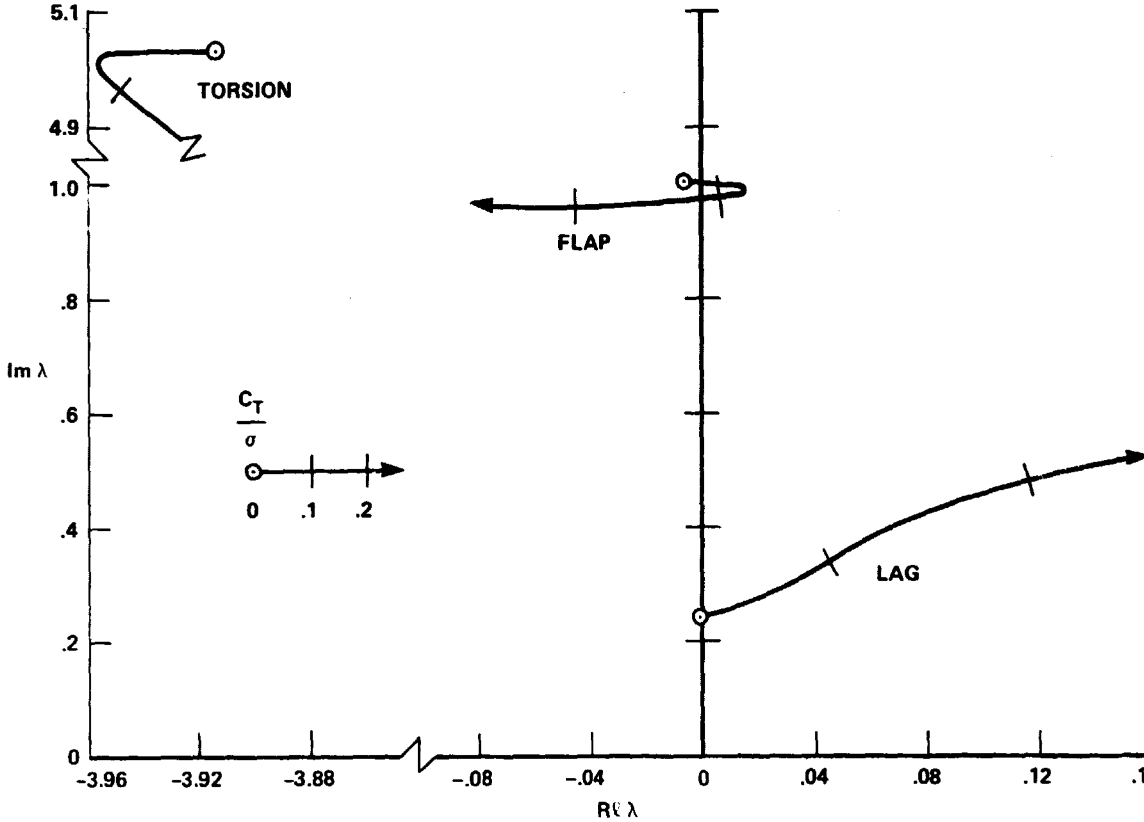

Figure 6.- Root loci for a single strip blade for ω_θ = 0 and X_{A_e} = .12c

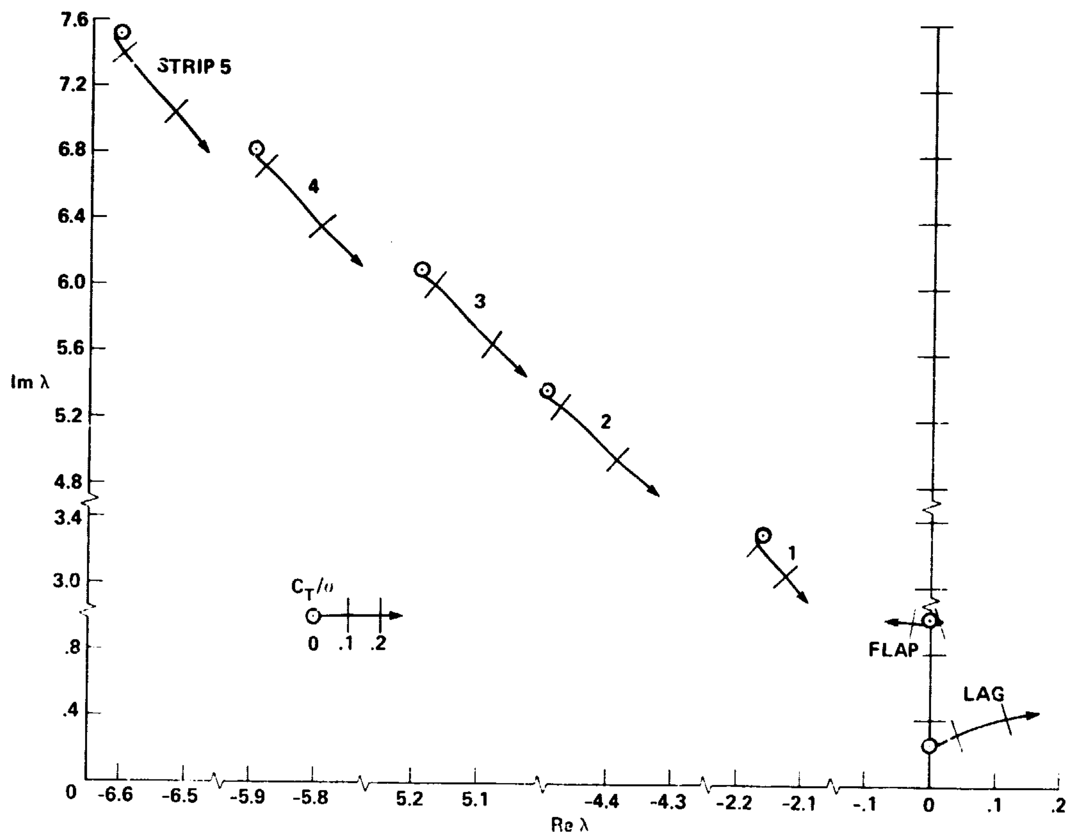

Figure 7.- Root loci for a constant lift rotor (5 strips) blade for $\omega_\theta = 0 \quad X_{A_e} = .12c$

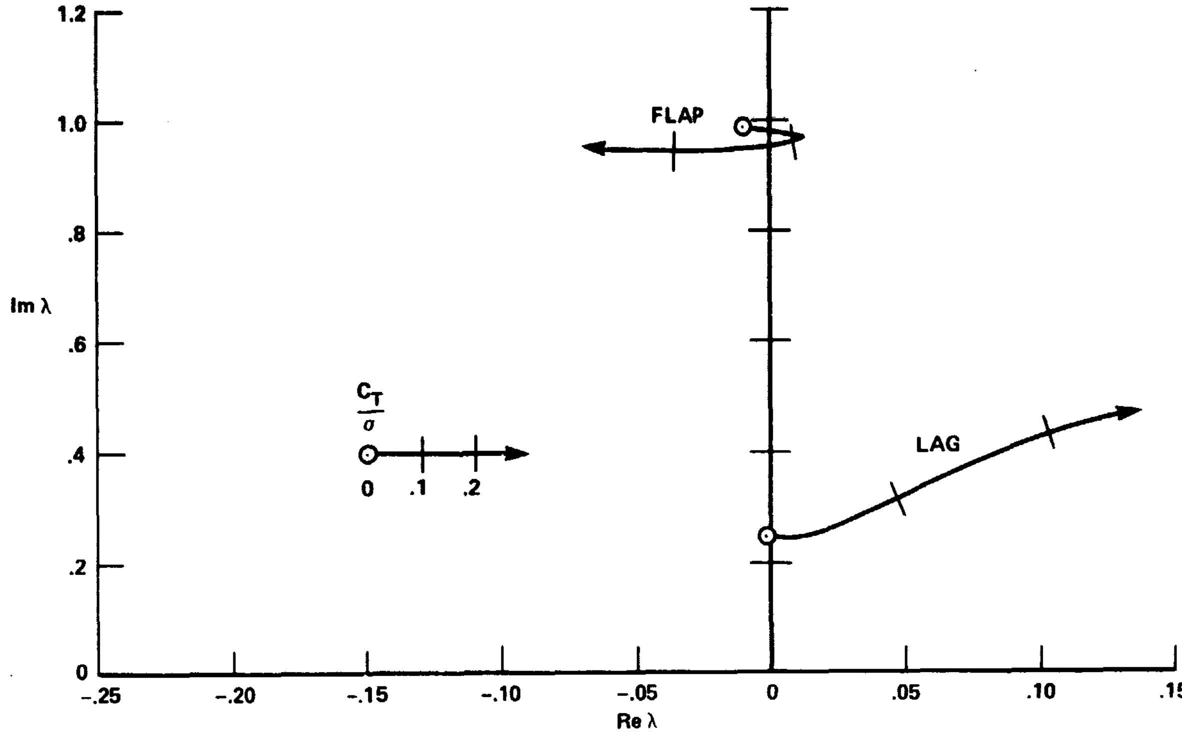

(a) Elastic axis offset X_{A_e} = .06c

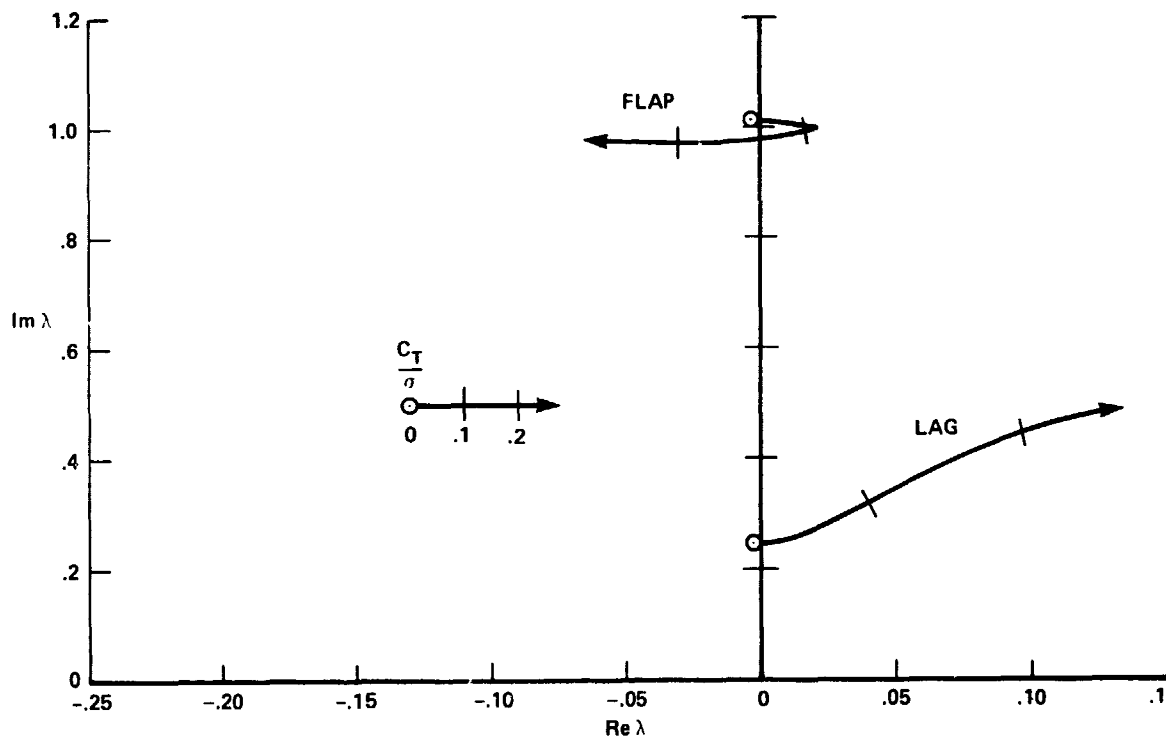

(b) Elastic axis offset X_{A_e} = .15c

Figure 8.- Flap and lag modes for ω_θ = 0

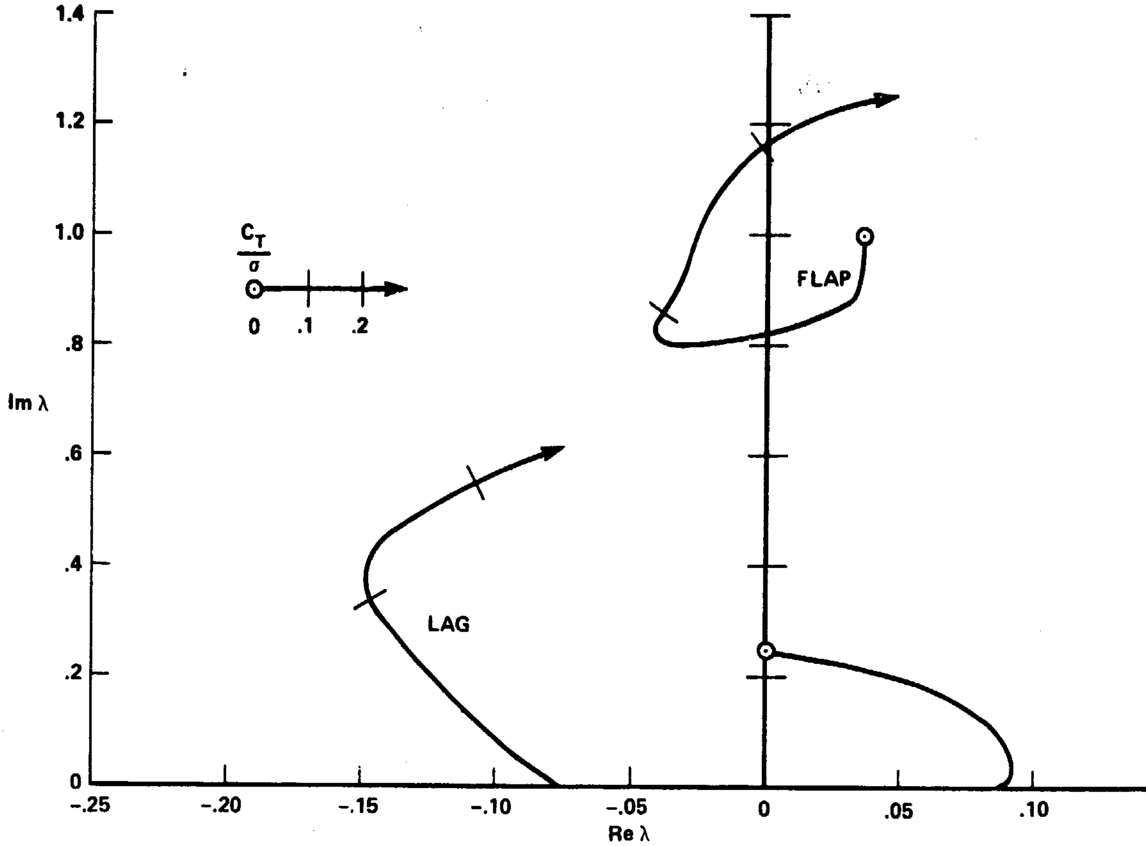

(a) C.G. offset from elastic axis X_{cg} = .12c (aft)

(c.g. coincidental with aerodynamic center)

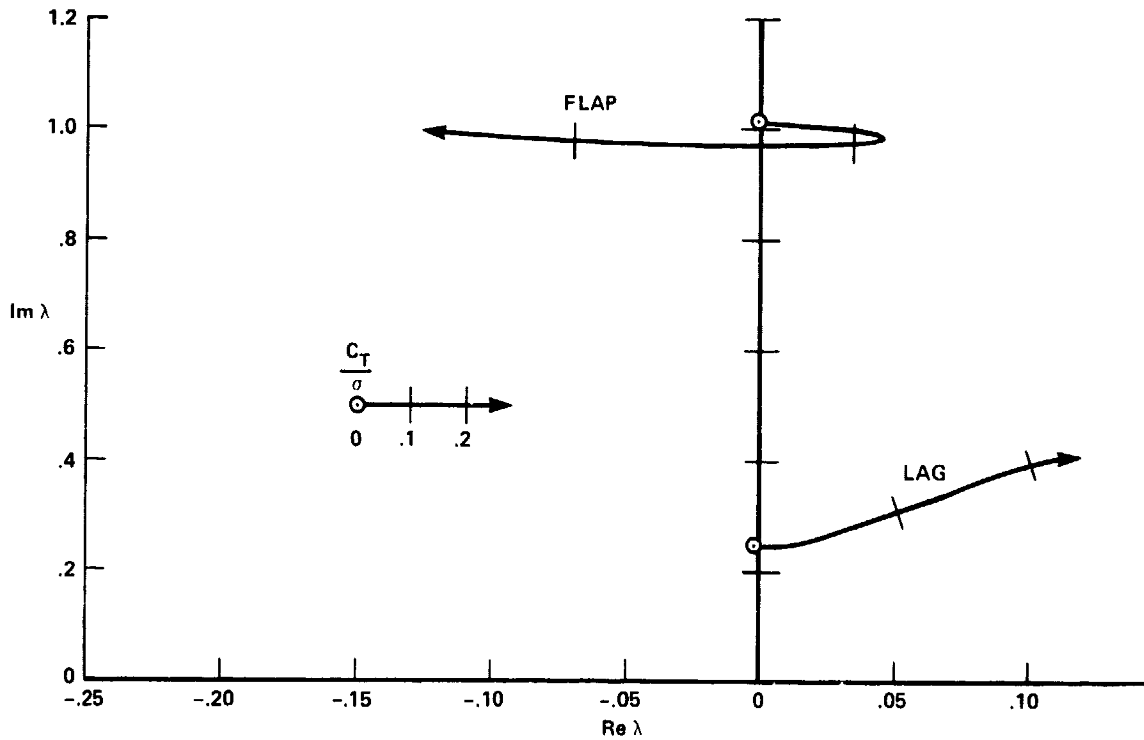

(b) C.G. offset from elastic axis X_{cg} = .06c (aft)

Figure 9.- Flap-lag roots for ω_θ = 0 and X_{A_e} = .12c

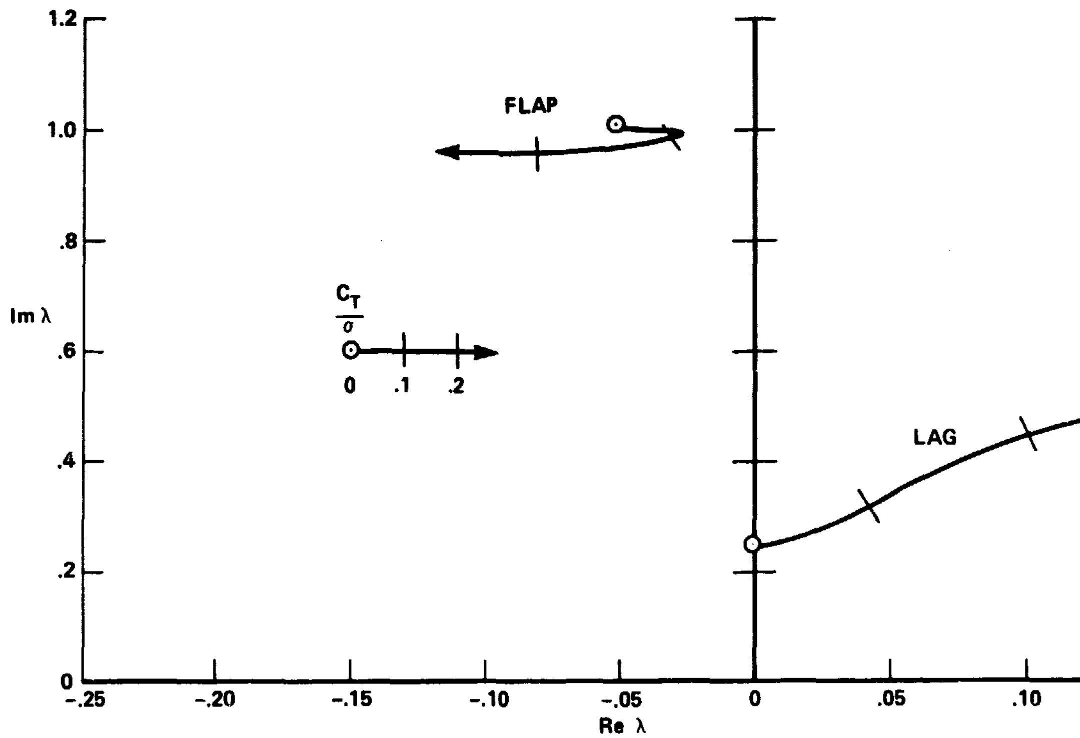

Figure 10.- Flap-lag roots for $\omega_\theta = 0$ and $X_{A_e} = .12c$ with flap structural damping ($g_\beta = .1$)

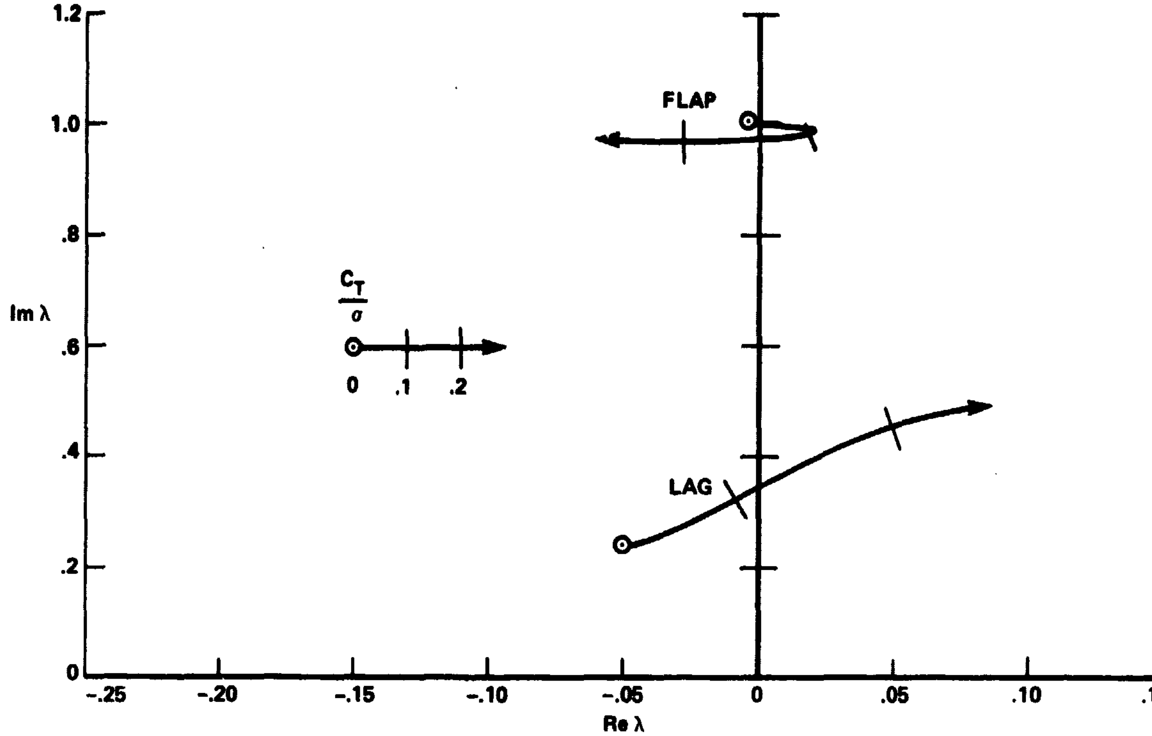

(a) Lag structural damping g_ζ = .1

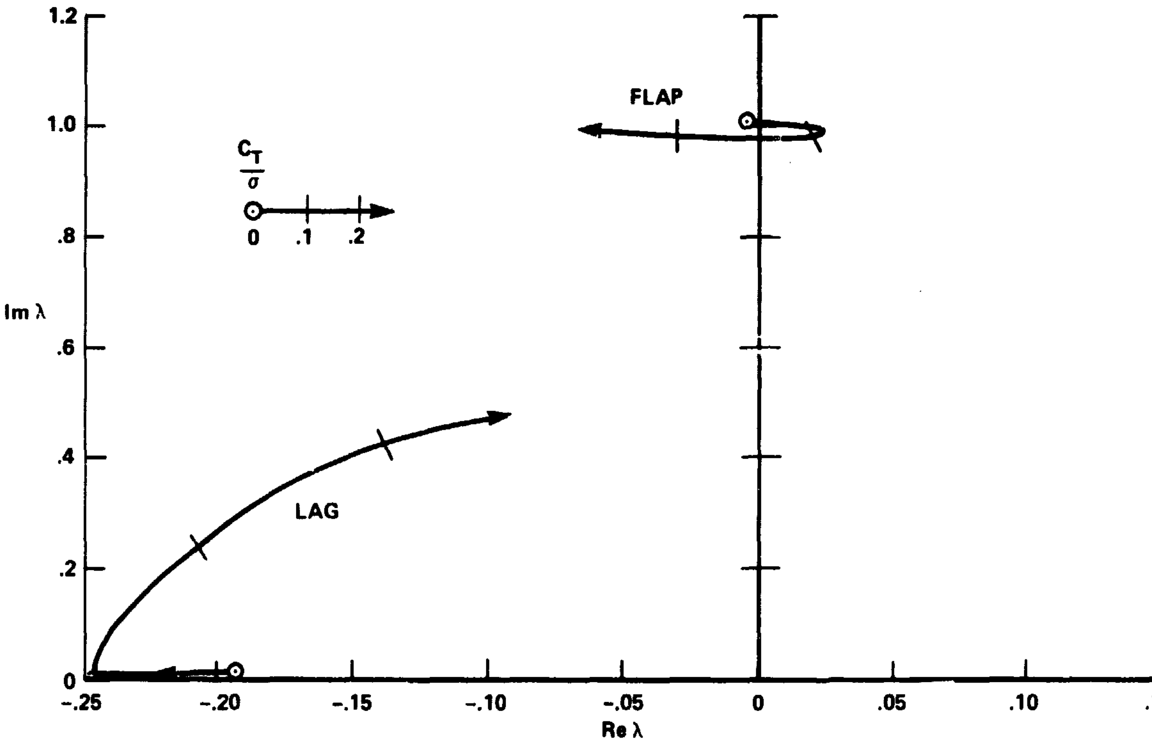

(b) Lag structural damping g_ζ = .5

Figure 11.- Flap-lag roots for ω_θ = 0 and X_{A_e} = .12c

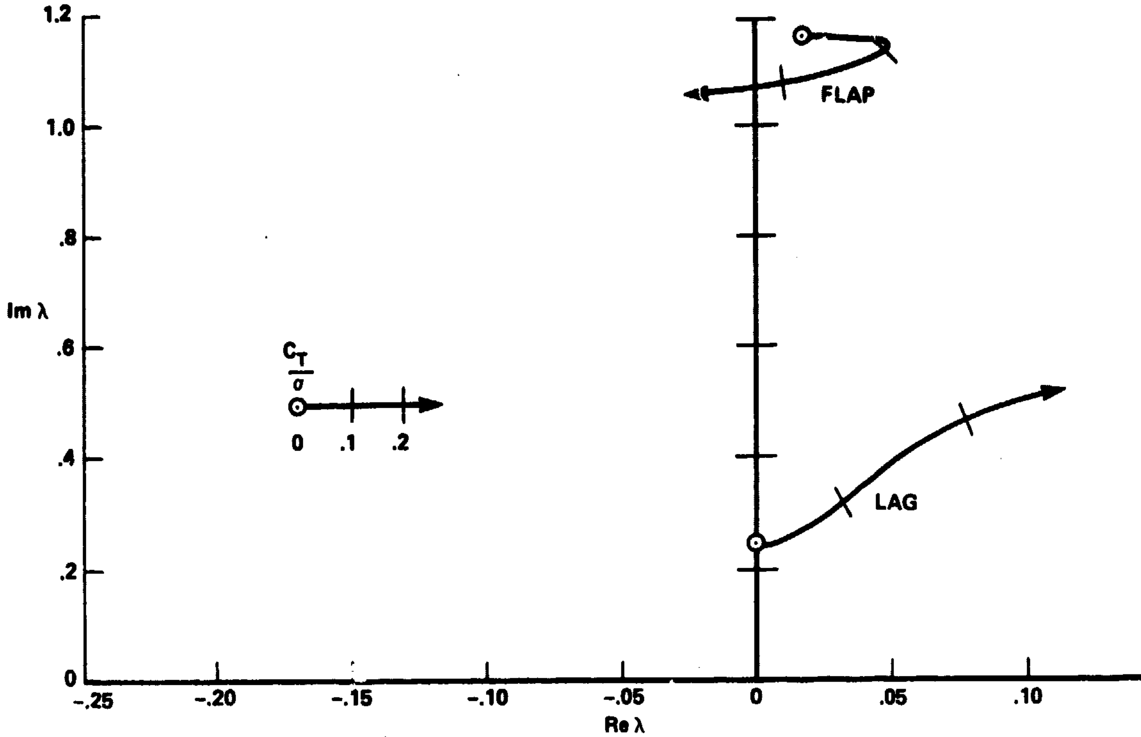

(a) Pitch-flap coupling R_β = .3.

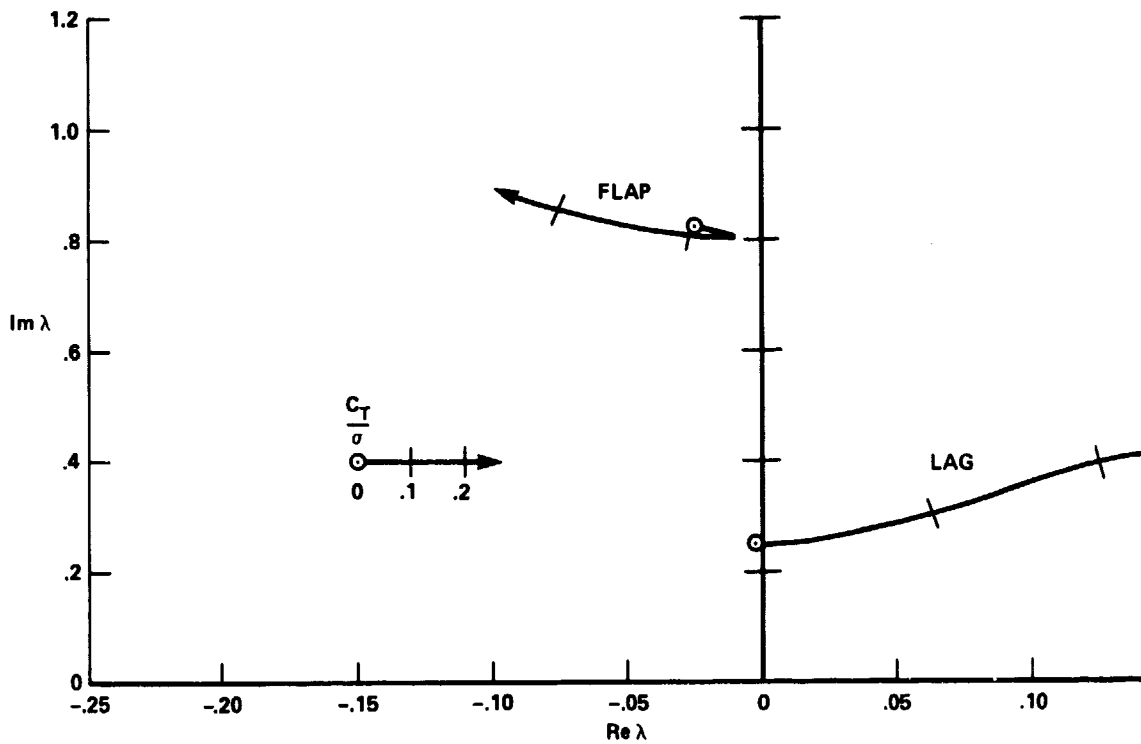

(b) Pitch-flap coupling R_β = -.3.

Figure 12.- Flap-lag roots for ω_θ = 0 and X_{A_e} = .12c.

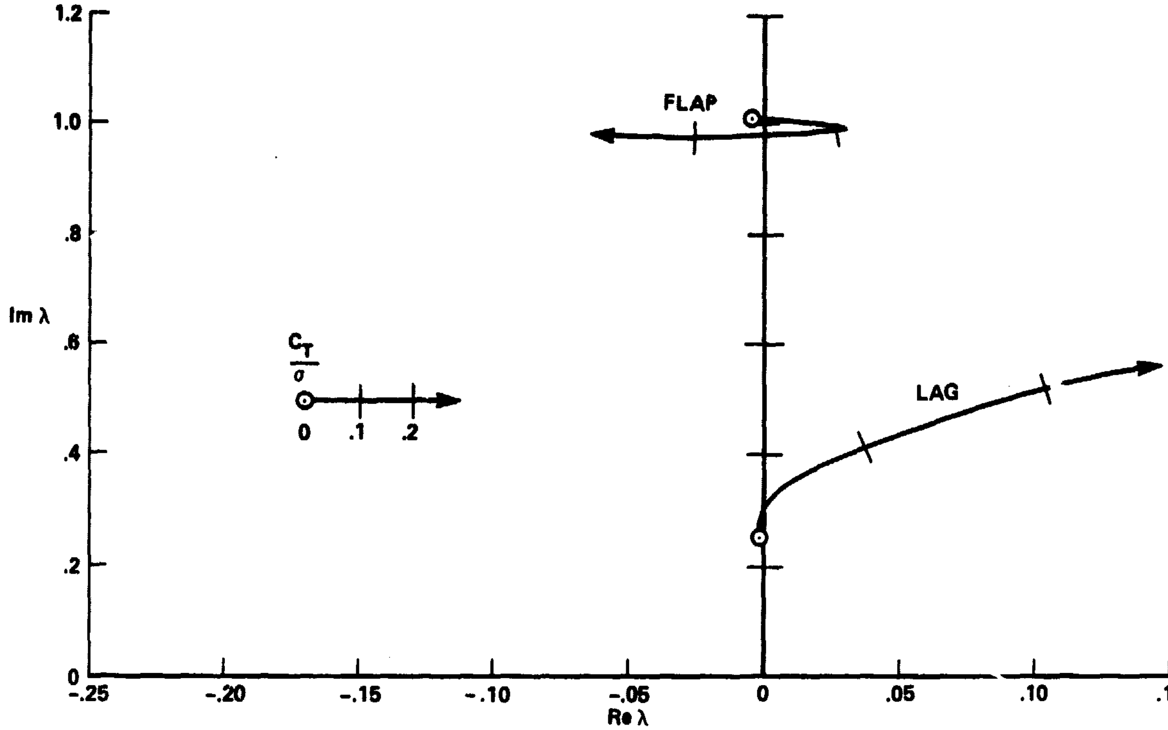

(a) Pitch-lag coupling $R_\zeta = .3$.

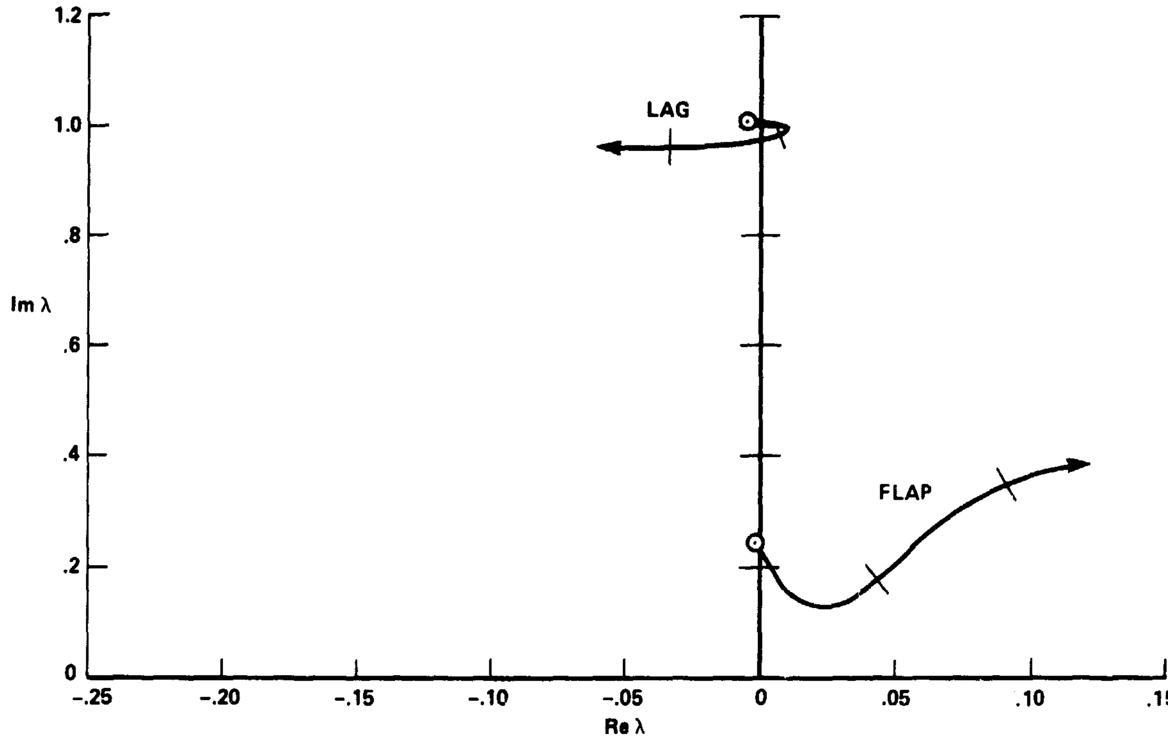

(b) Pitch-lag coupling $R_\zeta = -.3$.

Figure 13.- Flap-lag roots for $\omega_\theta = 0$ and $X_{A_e} = .12c$.

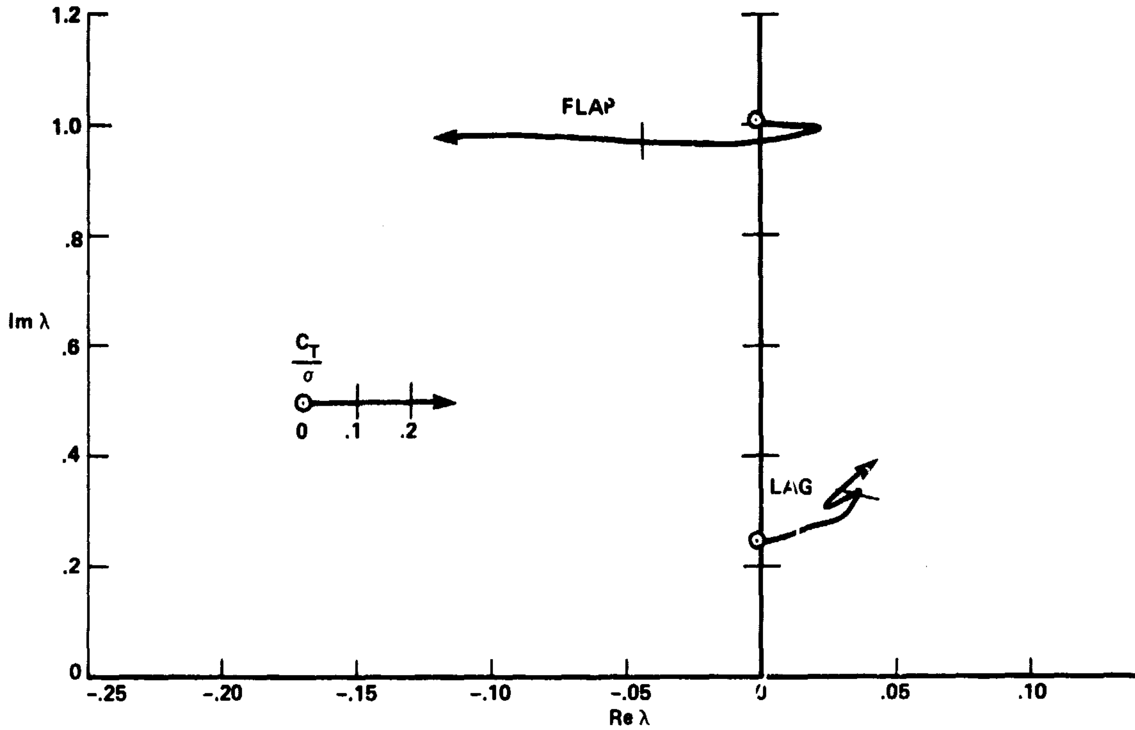

Figure 14.- Flap-lag roots for $\omega_\theta = 0$ and $X_{A_e} = .12c$ with tip Mach number $M_T = .6$ (compressibility effect).

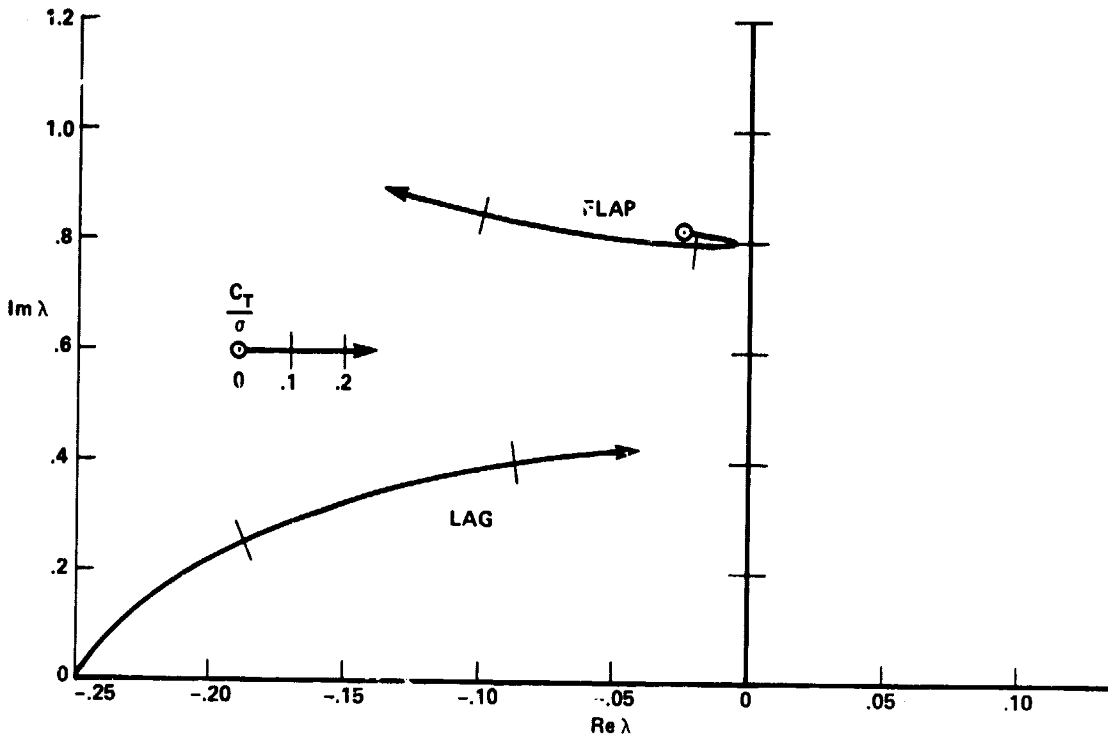

Figure 15.- Flap-lag roots for $\omega\theta = 0$, $X_{A_e} = .12c$, $R_\beta = -.3$.
and lag structural damping $g_\zeta = .5$.

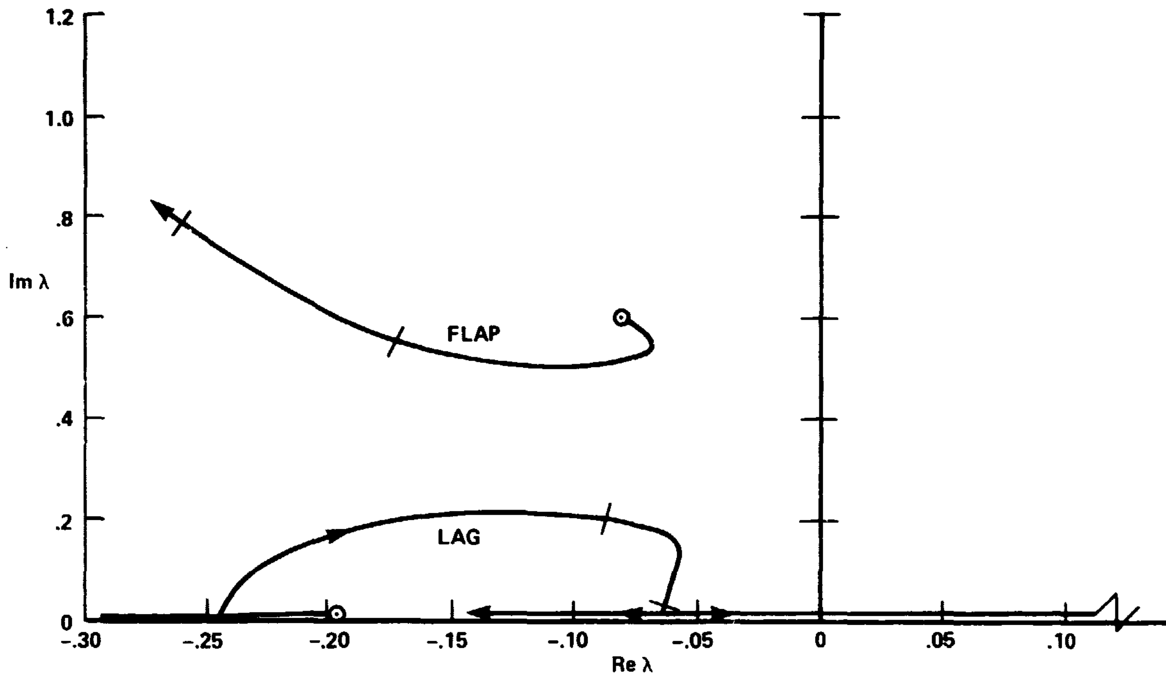

Figure 16.- Flap-lag roots for $\omega_\theta = 0$, $X_{A_e} = .12c$, $X_{cg} = .06c$, $R_\beta = .-3$ and structural lag damping $g_\zeta = .5$.